Dynamics of Shells

A seismic analysis of a modular shell system
Youssef BELMOUDEN, Pierino LESTUZZI, Souad SELLAMI (École Polytechnique Fédérale de Lausanne)*

Earthquake analysis of cylindrical roof shells
Shadi OSTAVARI DAILAMANI, James G. A. CROLL (University College London)*

Interpretation of seismic response of cylindrical roof shells
Shadi OSTAVARI DAILAMANI, James G. A. CROLL (University College London)*

Dynamic cylindrical shell equations by power series expansions
Anders M. HÄGGLUND, Peter D. FOLKOW (Chalmers University of Technology)*

Dynamic equations for a homogenous, fully anisotropic, elastic plate
Karl MAURITSSON, Anders BOSTRÖM, Peter D. FOLKOW (Chalmers University of Technology)*

For multiple-author papers:
Contact author designated by *
Presenting author designated by underscore

Proceedings of the 6th International Conference on
Computation of Shell and Spatial Structures
IASS-IACM 2008: "Spanning Nano to Mega"
28-31 May 2008, Cornell University, Ithaca, NY, USA
John F. ABEL and J. Robert COOKE (eds.)

A seismic analysis of a modular shell system

Youssef BELMOUDEN*, Pierino LESTUZZI, Souad Sellami, Youssef BELMOUDEN

*École Polytechnique Fédérale de Lausanne
Applied Computing and Mechanics Laboratory, ENAC-IS-IMAC, EPFL, Station 18, CH-1015, Lausanne, Switzerland
youssef.belmouden@epfl.ch

Abstract

This study deals with a new application of shell structures called modular shell system in seismic areas. This concept consists of an assemblage of tubular and cupola units. These structures are built using reinforced concrete and have been proposed for reconstruction after the Bam earthquake in Iran. A complete three-dimensional modal spectral analysis, including both horizontal and vertical ground acceleration components, with all probable load cases, is carried out. The results show that this structural concept behaves well under seismic loading. Nevertheless, more attention should be given for opening frame regions. Due to the profound and efficient structural performance of this shell concept, it is suggested as a housing system for areas where the local site effect increases the high seismic risk.

1. Introduction

A powerful earthquake occurred in the southeastern region of Iran on 26th December 2003. The magnitude of this event was reported to be 6.5 by USGS (Jafar Shoja-Taheri *et al.* [3]). The buildings in these regions were highly vulnerable even to moderate earthquakes and most of them completely collapsed when having been subjected to this earthquake. The reported project summarized in this paper is a contribution in the reconstruction effort after the Bam earthquake.

In this study, seismic analysis of a new concept of housing called modular shell system is presented (Dahinden [1]). This system is based on a shell concept known as differentiated shell construction. It consists of a medium tubular main unit as a cylindrical structure, and a number of cupola units or monolithic domes that are connected to the cylindrical main unit. It is well known that shell structures gain their strength by virtue of the three dimensional development of their surfaces, which gives it the ability to carry external loads primarily through in-plane stresses rather than bending. In general, the internal forces and stress distribution in shell structures, and especially for domes, is spatial. Hence, complex structures under combined loading paths are relegated to the domain of numerical analysis. Then, a three-dimensional finite element model for seismic analysis is developed. A complete modal spectral analysis is performed using ANSYS finite element package software.

2. Description and modeling of the modular shell system

The concept is a one story concrete tubular and concrete cupolas modular system for housing (Figure 1). The suitability of this system for dense urban housing lies in its scale and possible spatial arrangements. The system offers an optimum flexibility; it can be erected as an individual or group of housing system. The cupola units are joined, according to need, around the tubular main unit. The connecting links between the tubular and cupola forms act as flexible joints. Therefore, both tubular and domes units are studied separately. The tubular and cupola unit dimensions for structural modeling are given in the reference (Belmouden *et al.* [1]). The cupola construction is a serie of layers that are applied to the framework. The first and inner layers are of a gypsum/clay mixture and serves to stabilize the framework. The second layer consists of a conventional reinforced mortar-spray and the third and final layer, protecting against water and air erosion, are a plastic-film with 300% flexibility (Belmouden *et al.* [1]).

Both, tubular and dome units have no bearing walls. This allows the subdivision of these units into a number of partitions. The foundation and floor system is a poured on site concrete slab with mesh reinforcement (cast in situ). The structures are assumed to be rigidly connected to the floor foundation. So that, the dome and tubular units are considered to have continuous support.

The so-called Mindlin finite element is used for the structural analysis. The finite element model is a 3D shell element with both bending and membrane capabilities. Both in-plane and normal loads are permitted. The element has six degrees of freedom at each node: translations in the nodal x, y, and z directions and rotations about the nodal x, y, and z-axes. The analysis of the shell system material is based on the assumption that the material is linearly elastic, isotropic and homogeneous (Belmouden *et al.* [1]).

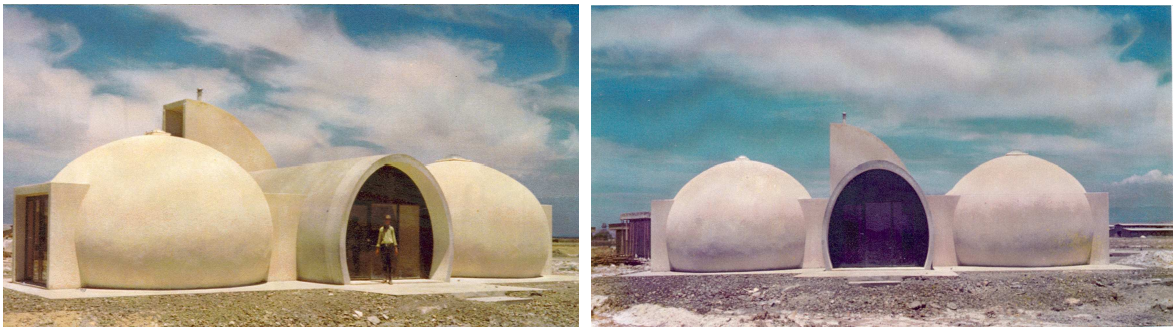

Figure 1: Different views of the modular shell system for housing

3. Response spectrum analysis

The type of the analysis performed is a complete response spectrum (Belmouden *et al.* [1]). The method involves the calculation of only the maximum values of the displacements and members in each mode using smooth design spectra according to the Eurocode EC8. The analysis deals with a three-dimensional calculation of mode shapes and natural frequencies for the undamped free vibration response of the structure. The selected modal analysis method is full subspace. For each principal direction, the square-root-of-sum-of-the-squares mode combination method is used. Figure 2 shows the period variations for the most significant modes of vibration to the negligible ones for both tubular and cupola units. The selected dominant modes are then represented in the design spectrum (Figure 2) (Belmouden *et al.* [1]).

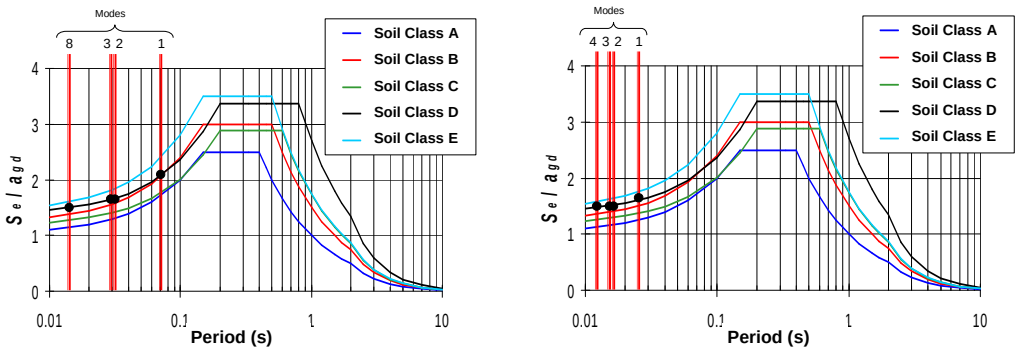

Figure 2: Tubular (left) and dome (right) units periods corresponding to the soil class D according to the Eurocode EC8 elastic spectrum

4. Results of the analysis

Three consecutive modal spectrum analyses were performed along the three principal directions. In the both horizontal directions, we have used the same spectrum excitation (same PGA). However, in the vertical direction, a reduction of 70% in the PGA value is adopted according to the Eurocode EC8.

The spectrum combination was performed for 63 load cases. The load cases are defined to represent the response produced by 100% of the lateral input spectrum in one direction and 30%, 70% and 100% in the other directions with negative and positive signs respectively. The maximum positive and negative values are obtained for the load case 11 (SW+Sy+Sx+Sz) and load case 18 (SW-Sy-Sx-Sz) respectively, where SW represents the self weight response; Sx, Sy and Sz are modal responses in the three principal directions. In the case of the dome unit, additional load cases such as SW+0.3Sz+0.3Sy, SW±0.3Sz±0.3Sy are necessary due to the geometrical form of the structure (Belmouden *et al.* [1]).

For the tubular unit, the maximum absolute horizontal displacements are equal to 1.4mm in X-direction and 0.0687mm in Z-direction. The maximum absolute vertical displacement is equal to 0.657mm. It is evident that the X-direction is the weakest one, while the Z-direction is the strongest.

The out-of-plane shear forces are negligible in comparison with the membrane forces. The bending and the twisting moments are very low. However, in-plane shear force could not be negligible. This confirms the membrane resisting mechanism developed in shell structures. Figure 3 shows that the highly stressed zones are always in the vicinity of the opening frames.

For concrete, the tension and compression strength conditions are checked: Maximum absolute principal (compression) stress σ_1: 7323(kN/m^2)>2900(kN/m^2). Maximum absolute principal (tension) stress σ_3: 1550 (kN/m^2)<<38000(kN/m^2). These tensile stresses represent a relevant parameter to determine the most probable cracking pattern in the structural units. As expected, the shell structure exhibits a very good behavior under compression.

For dome units (including opening frame regions), the maximum absolute horizontal displacements are equal to 0.097mm in X-direction and 0.19mm in Z-direction. The maximum absolute vertical displacement is equal to 0.30mm. The dome unit is more deformable horizontally in Z-direction that represents the weakest one, while the X-direction is the strongest. Both tubular and dome units do not exhibit the same weakest direction with respect to the location of the openings that can affect strongly the seismic behavior of the entire structure. The structure have to be correctly separated by flexible joints. We can arrive at the same conclusions as tubular unit concerning the in-plane shear force, the out-of-plane shear forces, the membrane forces, the bending and twisting moments. Figure 4 shows that the highly stressed zones are exclusively confined inside and near the opening frames.

The dome unit exhibits much better behavior in comparison with tubular unit. The dome unit presents a uniform distribution of stresses in the cupola region. The maximum drift in the tubular-dome connection is governed by the tubular deformation in the X-direction. The dome is more rigid than tubular unit in the X-direction.

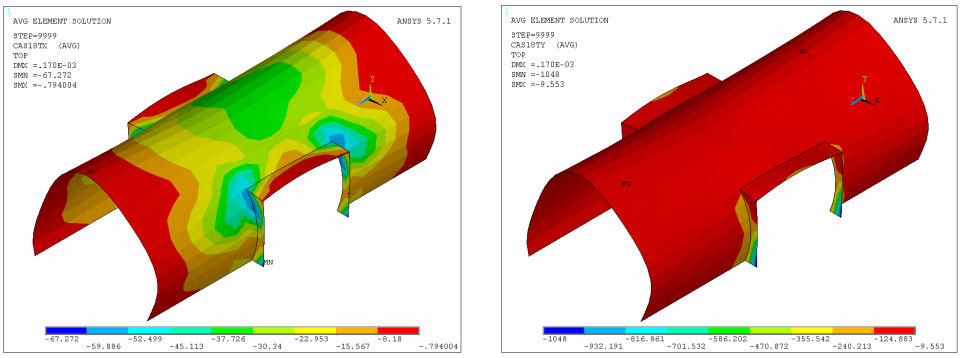

Figure 3: Membrane normal forces in x-element direction T_x (left) and in y-element direction T_y in load case 18 (right)

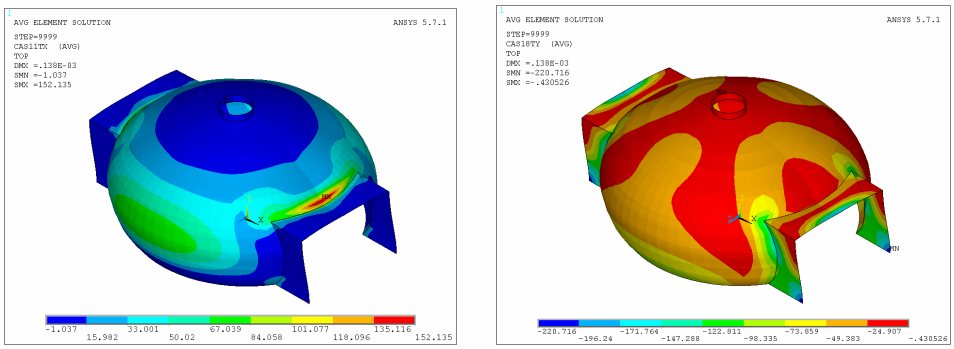

Figure 4: Membrane normal forces in x-element direction T_x in load case 11 (left) and in y-element direction T_y in load case 18 (right)

5. Conclusions

A new application of a system for housing based on shell concept is presented. The system is convenient for areas of high seismic risk. A three-dimensional finite element analysis was performed to assess the seismic performance of the structural system subjected to earthquake actions. Both the tubular and dome units exhibit a very low period of vibration. The structure is not sensitive to the ground acceleration amplification effect. So that, both tubular and dome units exhibits a uniform stress distribution. However, special attention is required for opening frame regions. In these regions, high membrane stresses are essentially confined in small zones. On the other side, stress concentrations are observed exclusively in the opening frames. However, the dome unit exhibits very good behavior under compression. The tension stresses are found very small.

In general, we have observed that the bubble system can carry the external seismic actions exclusively by membrane mechanism. Globally, both tubular and cupola units can be considered as free of bending effect. Membrane reinforcement is sufficient. However, the bending and shear distribution are developed in some regions to satisfy the global equilibrium and deformation requirements. The bending and shear field tend to be localized and confined to some regions in the vicinity of loading, geometrical discontinuities and deformation incompatibilities such as opening connections and units base regions. Finally, very satisfactory behavior under seismic actions is observed for the shell system of housing. We can conclude that the proposed system for housing can be recommended as a housing system for regions with a high seismicity.

References

[1] Belmouden Y., Lestuzzi P. A modular shell system for housing, *International Journal of shell and Spatial Structures*, April 2007, **48**: 19-27.

[2] Dahinden J., Architecture, Karl Krämer Verlag Stuttgart / Zürich, ISBN 3-7828-1601-3, 1987.

[3] Jafar Shoja-Taheri et al., The 2003 Bam, Iran, Earthquake : An interpretation of the Strong Motion Records, *Journal of Earthquake Spectra*, 2005; **21**: S181-S206.

Proceedings of the 6th International Conference on
Computation of Shell and Spatial Structures
IASS-IACM 2008: "Spanning Nano to Mega"
28-31 May 2008, Cornell University, Ithaca, NY, USA
John F. ABEL and J. Robert COOKE (eds.)

Earthquake analysis of cylindrical roof shells

Shadi OSTOVARI DAILAMANI*, James G. A. CROLL

*University College London (UCL)
Gower Street, London WC1E 6BT, UK
s.dailamani@ucl.ac.uk

Abstract

There are indications that thin shells are once again becoming a popular option for roofs covering large column free spaces. Especially in seismically active regions, it is important to incorporate into the design, consideration of how they will respond to the effects of earthquake loading. There are surprisingly few past studies of the performance of roof shells in earthquakes.

This paper reports a verification study based upon two independent methods: a finite element solution and a newly developed analytical method. The analytical method adopts an explicit solution based upon the Love-Timoshenko strain-displacement relationships and employs a Lagrangian approach to the derivation of the equations of motion. For typical cylindrical shell roofs these equations of motion are solved to determine first, the spectra of natural vibration modes and, secondly, the forced vibration response when the shell is subject to synchronous vertical motions recorded from a typical earthquake record. The contributions of each mode to displacement, acceleration, and stress responses are investigated and advice given on the numbers of modes required in a finite element analysis to adequately capture the dynamic response of open circular cylindrical roof shells subject to earthquake loading.

1. Introduction

Shells are amongst the most efficient of nature's structures in terms of the strength-to-weight ratios. As a result shell structures have many applications in different areas of science and technology. This potential is again being recognized in the increasing adoption of thin shells as an efficient means of covering large spaces. Among the various types of behaviour of shells, the dynamic response is one of the most complex and in areas of high seismisity the one likely to exert a controlling influence on design. It is therefore surprising to find so few past studies seeking to understand how thin shell roof structures will respond to earthquake loading. Despite two reviews which summarize numerous past research programs dealing with the free vibrations of shells (Leissa [3] and Qatu [6]), there appears to be very little published on the earthquake response of cylindrical shell roofs. Yamada [7] studied latticed cylindrical roofs using an equivalent cylindrical roof shell, and Kunieda [2] investigated the elastic response of spherical domes and cylindrical roof shells subject to horizontal and vertical components of earthquakes. It is difficult to draw general conclusions from these limited studies. Any new contribution to the existing literature needs to be cross-checked to ensure its validity and numerical accuracy. Unfortunately, because some of the important parameters controlling behaviour were not reported in previous paper (Kuneida [2]), it is not possible to directly compare the results. Hence, there appears to be a need for an independently validated analysis approach.

The dynamic analysis of shell structures is often performed by use of finite element (FE) programs. But effective use of FE programs should be based upon a sound understanding of shell theories, and an understanding of the mechanics of shells as well as an insight into the basic concept of the analysis method. Using analytical methods to verify the FE program on simpler examples is an effective way to prevent possible errors from occurring when analysing more complicated problems. The analytical approach described briefly in the following is used to provide confidence in the use of FE programs and will be shown to help identify problems, which could otherwise be overlooked.

2. Analytical modeling of natural frequencies

An analytical model is developed for a thin, open cylindrical shell, of radius of curvature *R*, longitudinal length L_x=*L*, thickness *h*, and opening angle ϕ as shown in Fig 1. Material is taken to be linearly elastic, and the damping ratio is taken to be constant in all modes. The strain-displacement relationships are based on those of Love and Timoshenko [3], together with the usual assumptions of thin shell theory.

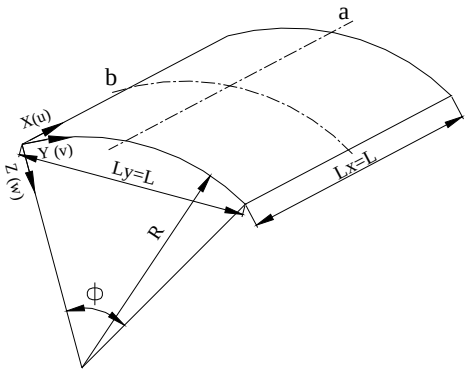

Figure 1: Geometry of shell

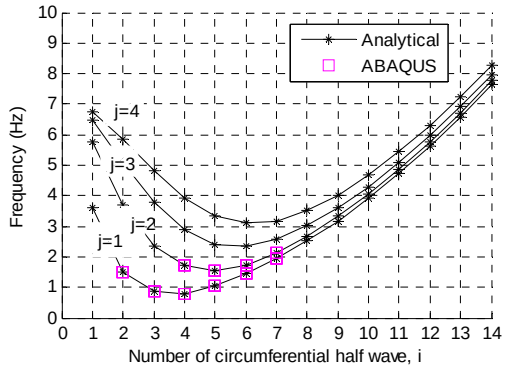

Figure 2: Comparisons of analytical and ABAQUS natural frequencies

The equations of motion for a shell undergoing a free vibratory motion, where the damping is neglected, are derived by Euler-Lagrange equations. For deriving the exact solutions for natural vibration modes from the differential equations of motion a spatial displacement pattern is taken in the form of double trigonometric series

$$u(x,y,t)=\sum_i\sum_j \bar{u}_{ij}\cos\frac{j\pi x}{L}\sin\frac{i\pi y}{R\phi}q_{ij}(t),\quad v(x,y,t)=\sum_i\sum_j \bar{v}_{ij}\sin\frac{j\pi x}{L}\cos\frac{i\pi y}{R\phi}q_{ij}(t),\quad w(x,y,t)=\sum_i\sum_j \bar{w}_{ij}\sin\frac{j\pi x}{L}\sin\frac{i\pi y}{R\phi}q_{ij}(t) \tag{1}$$

each mode of which satisfies the condition of simple supports.

$$v=w=0,\ N_x=M_x=0 \quad at\ x=0,L \qquad \text{and} \qquad u=w=0,\ N_\theta=M_\theta=0 \quad at\ y=0,R\phi \tag{2}$$

In the modal forms of eqn (1), *(i,j)* represent the number of half waves in the circumferential and longitudinal directions respectively, and $\bar{u}_{ij}$, $\bar{v}_{ij}$ and $\bar{w}_{ij}$ are the coefficients determined by solving the eigenvalue problem.

The generalized time response, used for solving the eigen value problem, is taken as $q_{ij}(t)=e^{m\omega_{ij}t}$, where m^2= *-1*, and ω_{ij} is the natural radial frequency corresponding with the mode (*i,j*). The analytical method was found to predict frequency spectra identical with the results reported by Kuneida *et al.* [1]. In a second study the natural frequencies obtained using the analytical method were compared with results obtained using the FE programme ABAQUS. The analysis was again performed on an isotropic open cylindrical shell with simply supports at four edges as indicated by eqn (2). Shell and material properties for this study were $R/h=500$, $L_y/L_x=1$, $\phi=\pi/3$, $B=\rho hR/E=10^{-6}$, $\nu=0.3$. Convergence of the 10 lowest natural frequencies, using the FE method, was found to be adequate using a 30×30 mesh. The FE predictions are compared with the present analytical results in Fig 2. The close agreement provides confidence in the use of either method to predict the response of the shell in earthquakes.

3. Confirmation of earthquake dynamic response

Once the mode shapes and natural frequencies of the open cylindrical shell have been obtained, the dynamic response can be computed from the mode superposition analysis. The derivation of the equations governing the vibrations of open cylindrical shells follows the method outlined by the authors [4], with the resulting equations of motion written as

$$\frac{\partial^2 q_{ij}}{\partial t^2}+2\zeta_{ij}\omega_{ij}\frac{\partial q_{ij}}{\partial t}+\omega_{ij}^2 q_{ij}=\frac{P_{ij}}{M_{ij}} \qquad i,\ j=1,\ 3,\ 5,\ \ldots \tag{3}$$

where z_{ij} is the modal damping ratio. The modal mass $M_{ij} = \rho h \frac{LR\phi}{4}$, is constant in all modes, and the modal force P_{ij} is defined as

$$P_{ij}(t) = \int_0^L \int_0^{R\phi} (P_x(t)u_{ij} + P_y(t)v_{ij} + P_z(t)w_{ij})\,dx\ dy \tag{4}$$

In the present study the earthquake loading is considered to be an external force which is modelled in terms of modal forces using a Fourier series representation of the equivalent body forces (P_x, P_y, P_z).

3.1 Modal force

In modal analysis the external forces need to be represented in terms of their modal components. If it is assumed that the loading is symmetric about the lines *aa* and *bb* of Fig 1 then just the odd modes will contribute to the total response of the shell. When the shell supports are subject to a synchronized vertical earthquake acceleration record, a_g, the time dependent body forces are

$$P_z = \overline{P}\cos\left(-\frac{\phi}{2} + \frac{y}{R}\right), \quad P_y = \overline{P}\sin\left(-\frac{\phi}{2} + \frac{y}{R}\right) \tag{5}$$

where $\overline{P} = \rho h a_g$. Substitution of eqns (1) and (5) into eqn (4) permits the modal forces to be represented as

$$P_{ij}(t) = \rho h L R \phi a_g(t) \frac{(-1+\cos i\pi)(-1+\cos j\pi)(\overline{w} i\pi - \overline{v}\phi)}{j\pi(i\pi - \phi)(i\pi + \phi)} \cos\frac{\phi}{2} \tag{6}$$

For a particular earthquake record, $a_g(t)$, the modal loads of eqn (6) allow the modal displacements q_{ij} to be found from eqn (3).

3.2 Validation of predictions

The displacement and acceleration response of the shell, with natural frequencies summarized in Fig 2, undergoing a typical earthquake loading has been derived using the analytical solution and compared with the results of a FE analysis. This comparison involved the use of the lowest 10 modes for both the analytical and FE method. While these limited numbers of mode are adequate to compare these alternative methods, it should be noted that the results are not fully converged. Maximum absolute displacement and acceleration responses of the shell over the earthquake duration are plotted in Fig 3 along center-line *bb*. Both the analytical and FE methods are solved using the time history modal analysis. The vertical component of the Landers earthquake [5], measured on June 28th 1992 at the Lucerne station with a duration of 48.12 s, Peak Ground Acceleration (PGA) of 0.818 *g* and 0.005 *s* time intervals of recorded data, was chosen as earthquake input. For convenience a constant damping ratio equivalent to 0.05 was considered for each mode. The analyses showed that the FE and analytical results summarized in Fig 3 (a) and (b) are in excellent agreement.

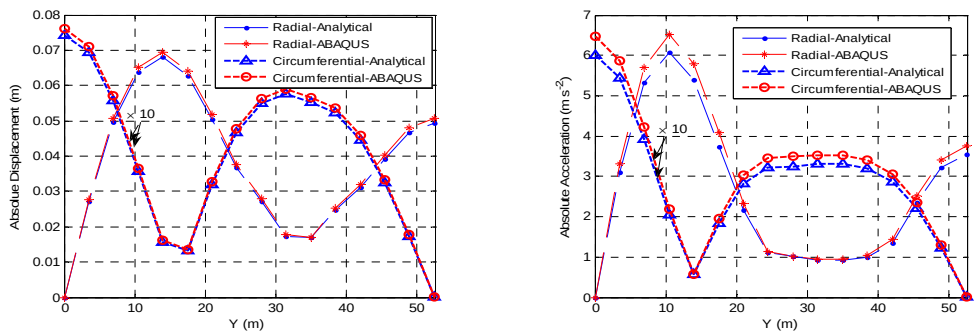

(a) Displacement (b) Acceleration

Figure 3: Displacement and acceleration along half width of b-b

3.3 Convergence with mode numbers

Of practical importance are the numbers of modes required for accurate prediction of displacement, acceleration, stress, etc. for a specific geometry of shell. Fig 4 (a) and (b) summaries the results of a study in

which the predictions are plotted against the numbers of modes included in the analysis. Modes are included in rank order, starting from that of the lowest frequency. The geometry is again chosen as that adopted for Fig 2, and 3. The displacement and acceleration results appear to have converged when 20 modes are included. But as can be seen from Fig 4 (a) there is a sudden jump in the response when mode 25 is included, with the response then showing no real change for increasing numbers of included modes. The reason for this jump is that mode 25 corresponds with mode *(i,j)=(1,1)* which has the highest level of modal force.

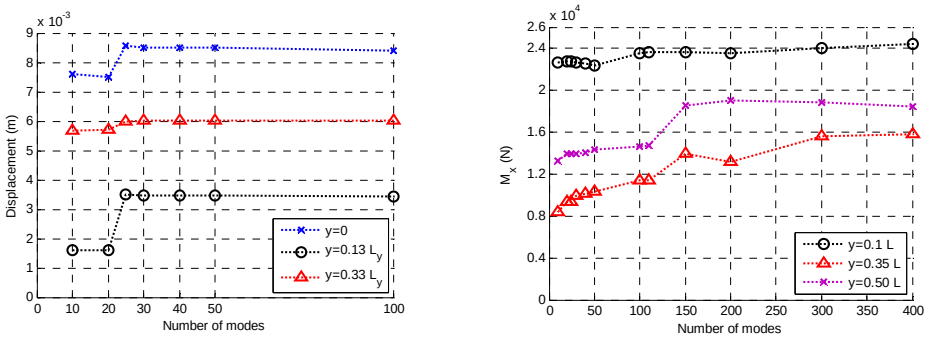

(a) Circumferential displacement (b) Bending stress

Figure 4: Convergence study at selected points along line b-b

4. Discussion and conclusion

The dynamic equation of motion for the vibration of open cylindrical shell with a constant damping ratio are developed. The governing natural frequencies are verified by favourable comparison with the previously reported results (Kuneida [2]). Both the analytical method and the FE method have shown clear agreement, increasing confidence in the use of either approach. For typical earthquake loading, convergence studies on the number of modes required in the modal analysis suggest that a detailed analysis should be performed to ensure the adequacy of numbers of modes considered in the response analysis of the shell. Were just a FE analysis to have been undertaken on the example shell chosen, the apparent convergence of behaviour with fewer that 25 modes could have discourage the analyst to include additional modes; the result might have been a serious misrepresentation of the earthquake response, especially those stresses related to in-plane displacements.

The analytical method can be conveniently used to answer practical question such as: the effect of in-plane modes in the response of the shell; participation of different modes in the displacement, acceleration and stress responses; the effect of damping in the total response of the shell; and the comparison between the effects of horizontal and vertical component of earthquake in the response of the shell. While the FE is less convenient for such studies it has the considerable advantage of allowing more complex shell problems to be analysed.

References

[1] Kunieda, H and Kitamura, K and Ohya, T. Free vibration and JMA-earthquake responses of cylindrical roofs. *Annual Disaster prevention research institute*, (39):B-1, 1996.

[2] Kunieda, H. Earthquake Response of Roof Shells. *International Journal of Space Structures*, 12:149-160, 1997.

[3] Leissa, A.W. *Vibration of shells*. NASA, 1973.

[4] Ostovari Dailamani, S and Croll, J G A. Dynamic analysis of cylindrical roof shells for earthquake resistance design. to be peresented at *The 9th International Conference on Computational Structures Technology*, Greece, 2008.

[5] PEER Strong Motion Database. http://peer.berkeley.edu/smcat/.

[6] Qatu, M.S. Recent research advances in the dynamic behavior of shells: 1989--2000, Part 2: Homogeneous shells. *Applied Mechanics Reviews*, 55:415, 2002.

[7] Yamada, S. Vibration behavior of single-layer latticed cylindrical roofs. *International Journal of Space Structures*, 12:181--190, 1997.

Proceedings of the 6th International Conference on
Computation of Shell and Spatial Structures
IASS-IACM 2008: "Spanning Nano to Mega"
28-31 May 2008, Cornell University, Ithaca, NY, USA
John F. ABEL and J. Robert COOKE (eds.)

Interpretation of seismic response of cylindrical roof shells

Shadi OSTOVARI DAILAMANI*, James G. A. CROLL

*University College London (UCL)
Gower Street, London WC1E 6BT, UK
s.dailamani@ucl.ac.uk

Abstract

Of the limited past investigations of how thin shell roofs respond to earthquakes, attention has been restricted to consideration of just the out-of-plane modes, with the contributions from the in-plane modes generally being neglected. This paper reports a study investigating the importance of these in-plane modes to the dynamic response of open-circular cylindrical roof shells subject to earthquake loading. The contributions of each mode to the displacement, acceleration, and stress responses are investigated, showing that certain, normally neglected modes, can have considerable influence on the predicted response. The relative importance of vertical and horizontal components of earthquake in the dynamic response of cylindrical shell are also investigated.

1. Introduction

Despite the considerable research effort to understand the free vibration of shell structures there is little investigating the response to earthquake loading. In a previous paper the authors have developed an analytical method and checked its consistency against a FE program [3]; this provided confidence that the analytical method can be used to check a number of potentially important questions that have not so far been fully answered. For example, is it legitimate to use the same number of modes for the convergence of stresses as it is for displacements. Furthermore, the analytical method allows examination of the importance of the contributions of modes to the total dynamic response having different membrane and bending energy content. The participation of the in-plane modes and out-of-plane modes in the total response for each characteristic mode shape is another complexity of the shell structures behaviour. How these in-plane and out-of-plane modes interact, will be shown to influence the response of shell structures for different types of ground motion. In particular, earthquake spectra containing a dominance of high frequencies will be shown to have an important bearing on the shell modes that dominate the response spectra. An assessment of the relative importance of vertical and horizontal components of the earthquake motion in the displacement, acceleration, and stress responses of the shell will provide an illuminating study in this respect.

2. Analytical modeling

A thin open cylindrical shell of radius of curvature R, longitudinal length $L_x=L$, thickness h, and angle ϕ (Fig 1) is considered for the purpose of this study. The equation of motion is derived for a shell with simply supports at four edges as previously explained by the authors [2]. The Analysis is performed using the modal analysis with a constant damping ratio, using an approach that has been confirmed through comparisons with finite element analysis. The membrane and bending stresses are derived using eqn (1), in which extensional stiffness $K = Eh(1-\nu^2)^{-1}$, flexural stiffness $D = Eh^3(1-\nu^2)^{-1}/12$, E =modulus of elasticity, ν =Poisson's ratio, and u, v are the axial, circumferential (in-plane) displacement, and w is the lateral (out-of-plane) displacement. The horizontal earthquake acting normal to the axis of the shell, is derived using the procedure explained in reference [2] in relation to the vertical component of earthquake. For the horizontal earthquake component modal force can be represented as eqn (2), in which $\bar{v}_{ij}$, and $\bar{w}_{ij}$ are the non-dimensional coefficient determined by solving the eigenvalue problem.

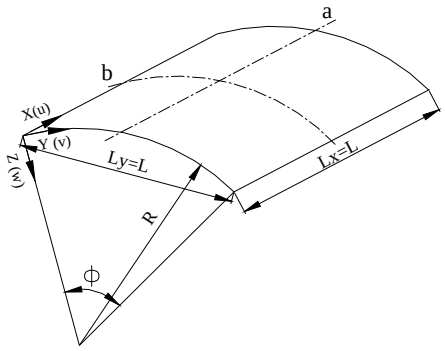

$$N_x = K(\frac{\partial u}{\partial x} + \nu\frac{\partial v}{\partial y} + \nu\frac{w}{R}),\ M_x = D(-\frac{\partial^2 w}{\partial x^2} - \nu\frac{\partial^2 w}{\partial y^2} + \frac{\nu}{R}\frac{\partial v}{\partial y})$$

$$N_y = K(\frac{\partial v}{\partial y} + \frac{w}{R} + \nu\frac{\partial u}{\partial x}),\ M_y = D(-\nu\frac{\partial^2 w}{\partial x^2} - \frac{\partial^2 w}{\partial y^2} + \frac{1}{R}\frac{\partial v}{\partial y}) \quad (1)$$

$$N_{xy} = K\frac{1-\nu}{2}(\frac{\partial u}{\partial y} + \frac{\partial v}{\partial x}),\ M_{xy} = -D(1-\nu)(-\frac{\partial^2 w}{\partial x \partial y} + \frac{1}{R}\frac{\partial v}{\partial x})$$

Figure 1: Geometry of shell

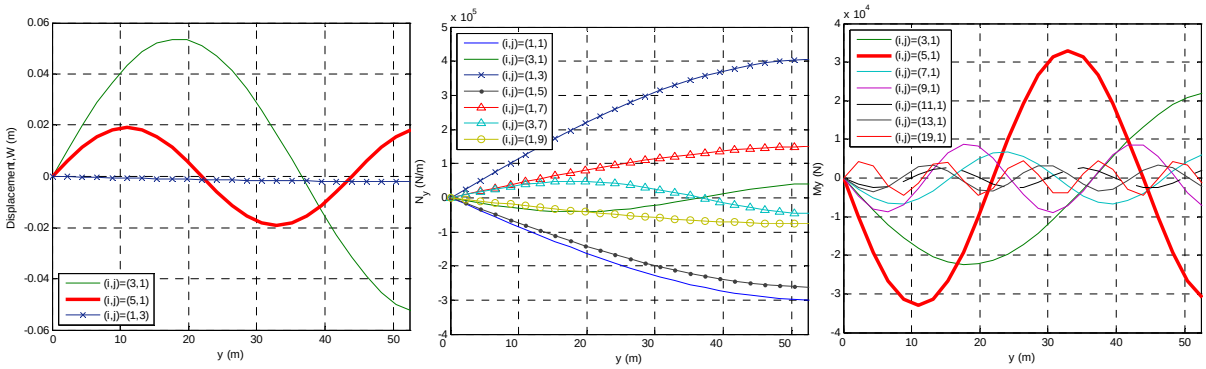

(a) Radial dispalcement (b) N_y (c) M_y

Figure 2: Modal contribution of displacement, membrane and bending stress resultants at $x = L_x/2$

$$P_{ij}(t) = \rho h L R \phi a_g(t) \frac{(1+\cos i\pi)(-1+\cos j\pi)(-\overline{w}_{ij}\, i\pi - \overline{v}_{ij}\,\phi)}{j\pi(-i\pi+\phi)(i\pi+\phi)} \sin\frac{\phi}{2} \quad (2)$$

3. Importance of different modes in the response

The participation of different modes in the displacement response and their relationships with the modal participation in the stresses has been investigated for an isotropic cylindrical shell having *R/h=500, R=104.8 m,* L_x*=104.8 m,* $\phi = \pi/3$, $E=9.1\times10^{10}$ N/m^2, ρ = *4150.5kg/m*^{3}. For convenience the modal damping ratio was considered to be 0.05 for each mode. The time history modal analysis was carried out for the vertical component of the Landers earthquake on June 28th 1992 with data taken from Lucerne station. The earthquake had a period of *48.12 s*, with data available at each *0.005 s* time interval, and Peak Ground Acceleration *(PGA) = 0.818 g* [4]. The analysis was performed for a total of *19* circumferential half-waves and *9* axial half-waves. Using the analytical method the contributions of different modes in the displacement and stress responses of the shell, at the time of maximum response, are plotted in Fig 2 (a), (b), (c) for the half-width across the center-line *bb* ; the response is symmetric about the center-line *aa*. The results of the analysis showed that even though the maximum displacement may occur at particular time and location, that would not necessarily relate to the most severe stresses. Stresses have a very different modal participation. The nature of the modal participations in both the maximum displacement and stress response is strongly influence by the relationships between the natural frequency spectrum of the shell and the spectral energies of the earthquake. Therefore, depending on the relationship between the natural frequency spectrum and earthquake spectrum we could expect very different results. As it can be seen from the Fig 2 for a shell having $L_y/L_x=1$, $B = \rho hR/E = 10^{-6}$ s^2 the participation of different modes are not the same for displacements and stresses. The out-of-plane displacement is dominated by modes *(i,j)=(5,1), (3,1)*. Despite having a high modal loading in mode *(i,j)=(1,1)* the contribution of this mode toward the out-of-plane displacement is very small in comparison with its contribution to the in-plane displacements. In Fig 2 the importance of *(i,j)=(1,1)* to the membrane stress resultant N_y is a reflection of this

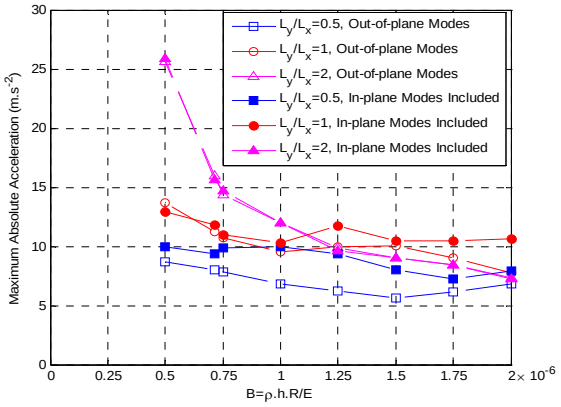

(a) Radial acceleration

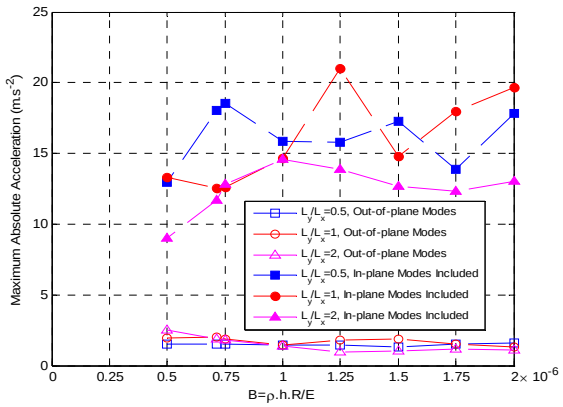

(b) Circumferential acceleration

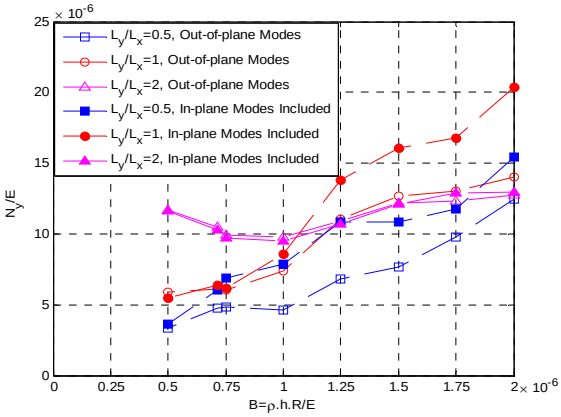

(c) N_y

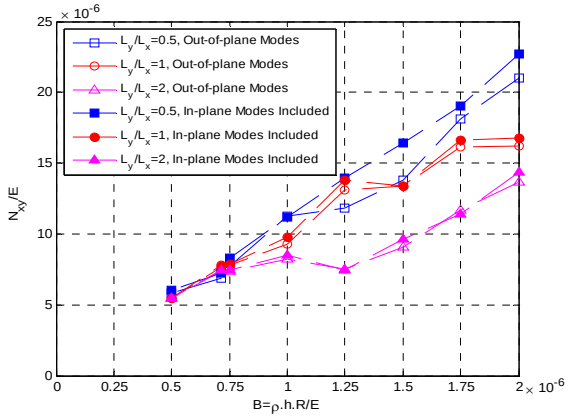

(d) N_{xy}

Figure 3: Acceleration, and membrane stress for vertical component of Landers earthquake

mode contribution to in-plane displacement, *v*, so it would be expected that ignoring mode *(i,j)=(1,1)* would result in higher error for in-plane displacements than out-of-plane displacements. There are very small contributions to the out-of-plane displacements from modes having shorter axial wavelengths. In contrast shorter wavelengths in both the axial and circumferential directions make significant contributions to the membrane and particularly the bending stresses as illustrated in Fig 2 (c).

4. Effect of in-plane modes in the response of cylindrical shell

For each choice of wave number *(i,j)* there are *3* natural frequencies. In the past just the out-of-plane modes (those for which the out-of-plane deformation, *w*, dominates) have been considered in the earthquake response of shells [1, 5]. However for each *(i,j)* there are two other modes within which one of the in-plane deformations *(u,v)* dominates. These are referred to here as in-plane modes. Although the in-plane modes generally correspond with frequencies an order of magnitude higher than those of the out-of-plane modes, there may be circumstances in which these modes could play an important role in the earthquake response of the shell. The effects of considering in-plane modes in the displacement, acceleration, and stress responses have also been investigated. The analyses were performed for a range of shells with *R/h=500*, $\phi = \pi/3$, $B = \rho h R / E$ between 0.5 to 2×10^{-6} s^2, and L_y/L_x=0.5, 1, 2. Having derived the out-of-plane and in-plane natural frequencies the responses are determined considering just the out-of-plane modes and compared with the responses when the effect of in-plane modes are also included. Analyses of shells under the vertical components of earthquake show that neglecting the effects of in-plane modes can result in considerable differences, particularly in the circumferential acceleration as shown in Fig 3 (*b*). In contrast these modes make little difference to radial and circumferential displacement as well as bending stresses. Because the membrane stresses are directly related to

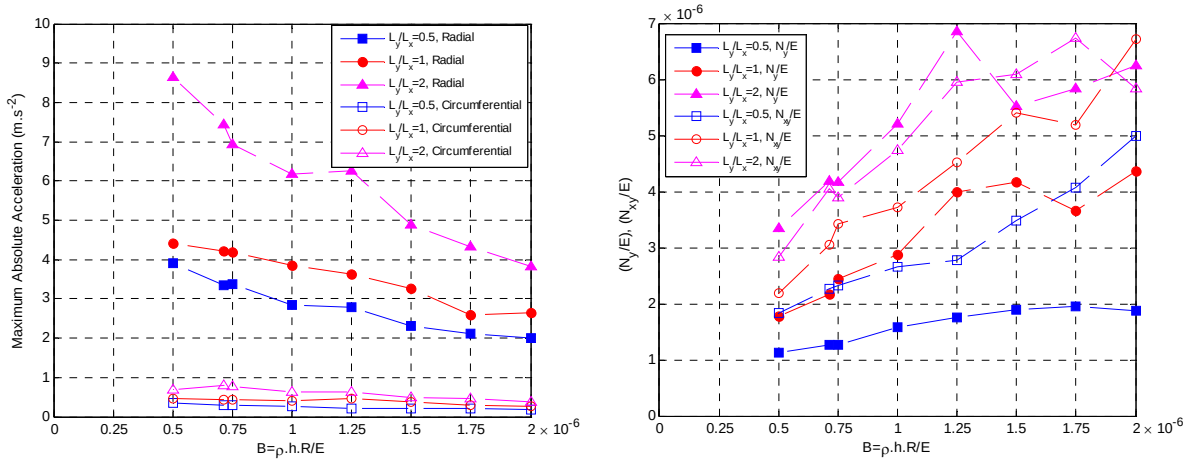

(a) Acceleration (b) Stress

Figure 4: Maximum absolute acceleration and stress for horizontal component of Landers earthquake (in-plane modes included)

the in-plane displacements it might be anticipated that the in-plane modes would be important in their determination. Fig 3 (*c*) shows that inclusion of the in-plane mode for a shell with $B=1.25 \times 10^{-6}$ s^2, $L_y/L_x=0.5$, $R/h=500$, $\phi = \pi/3$ results in almost *40 %* increase in N_y, and *15%* in N_{xy}.

5. Comparison of responses to vertical and horizontal component of earthquake

The horizontal component of the Landers earthquake is also used for investigating the effect of horizontal component of earthquake on Cylindrical roof shells. Again, the earthquake data is available for every *0.005 s* time interval, and *PGA=0.712g* [4]. The differences in response to vertical and horizontal components of Landers earthquake in the response of the shell can be seen by comparing Fig 3 with Fig 4. It is clear that the vertical component of Landers earthquake leads to higher displacement, acceleration, and stresses compared with the horizontal component of Landers earthquake. This suggests that consideration of the vertical component of earthquakes is very important in the design of this form of shell. For the horizontal component of earthquake, the inclusion of in-plane modes has a negligible effect on the predicted results but can be significant for the vertical components. However, as can be seen from Fig 4 the responses to horizontal earthquake components are more significantly dependent on the shell geometry and material properties so that this conclusion may need to be reassessed for shells with different opening angle, and thickness to radius ratio.

6. Conclusion

This study confirms that inclusion of the in-plane modes within the analysis of the seismic behaviour of cylindrical shell roofs can have substantial effects upon the predicted stresses. The results also confirm that the vertical components of earthquakes are likely to produce higher responses than those of the horizontal components.

References

[1] Kunieda, H. Earthquake Response of Roof Shells. *International Journal of Space Structures*, 12:149-160, 1997.

[2] Ostovari Dailamani, S and Croll, J G A. Dynamic analysis of cylindrical roof shells for earthquake resistance design. to be peresented at *The 9th International Conference on Computational Structures Technology*, Greece, 2008.

[3] Ostovari Dailamani, S and Croll, J G A. Earthquake analysis of cylindrical roof shells. to be peresented at *6th International Conference on Computation of Shell & Spatial Structures , Ithaca, 2008.*

[4] PEER Strong Motion Database. http://peer.berkeley.edu/smcat/.

[5] Yamada, S. Vibration behavior of single-layer latticed cylindrical roofs. *International Journal of Space Structures*, 12:181--190, 1997.

Proceedings of the 6th International Conference on
Computation of Shell and Spatial Structures
IASS-IACM 2008: Spanning Nano to Mega
28-31 May 2008, Cornell University, Ithaca, NY, USA
John F. ABEL and J. Robert COOKE (eds.)

Dynamic cylindrical shell equations by power series expansions

Anders M. HÄGGLUND, Peter D. FOLKOW*

*Department of Applied Mechanics, Chalmers University of Technology,
SE-412 96 Göteborg, Sweden

Abstract

Dynamics of an infinite circular cylindrical shell is considered. The derivation process is based on power series expansions of the displacement components in the radial direction. Using the three dimensional equations of motions, a set of recursion relations is identified expressing higher displacement coefficients in terms of lower order ones. The new approximate shell equations are hereby obtained from the boundary conditions, resulting in a set of six partial differential equations. These equations are believed to be asymptotically correct and it is, in principle, possible to go to any order. Dispersion curves, together with the eigenfrequencies for a 2D case, are calculated using exact, classical and expansion theories. It is shown that the approximate equations containing order h^2 are in general as good as or better than the established theory of the same order.

1 Introduction

The investigation of the governing equations for cylindrical shells has been of great interest in the history of elastodynamic theory, ranging from the exact three-dimensional theory to simplified approximate theories. In these simplified theories, both the dynamic equations and the boundary conditions are often derived using various kinds of simplifying kinematic assumptions. There is much debate on the correctness of these assumptions, and as the engineering demands increase continuously, resulting in more complex shell structures and the need for higher computational accuracies, it becomes more crucial to choose the most appropriate simplifications. This calls for a systematic approach when tackling the dynamic behavior of the shell structures in question, which is the main purpose of this presentation. Here, the method used is based on a series expansion technique. The displacement fields are expanded using power series in the thickness coordinate. Dispersion curves as well as the lowest eigenfrequencies in the 2D case of plane strain are given for exact, classical and expansion theories. The present method has previously been adopted for rods by Boström [1], plates by Boström *et al.* [2], and for piezoelectric layers by Mauritsson *et al.* [4].

2 Power series expansions

Consider a circular cylindrical shell with middle surface radius R and thickness h. The shell is homogeneous, isotropic and linearly elastic with density ρ and Lamé constants λ and μ. Cylindrical coordinates are used with radial coordinate r, circumferential coordinate θ and axial coordinate z. Along the axis of revolution of

the cylinder, coinciding with the coordinate axis z, the cylinder is infinite. The corresponding displacement fields are denoted u, v and w. Adopting the three-dimensional equations of motion gives

$$\mu\nabla^2\vec{u} + (\lambda+\mu)\nabla\nabla\cdot\vec{u} = \rho\,\ddot{\vec{u}}. \tag{1}$$

Introduce $r = R+\xi$ where $-h/2 \le \xi \le h/2$. To derive shell equations the displacement components are now expanded in power series in the thickness coordinate ξ

$$f = f_0(z,\theta,t) + \xi f_1(z,\theta,t) + \xi^2 f_2(z,\theta,t) + \ldots, \tag{2}$$

for $f = u, v, w$. Note that these expansions involve both even and odd powers of ξ as symmetric and antisymmetric motions with respect to ξ do not decouple.

Insertion of the expansions (2) into the equations of motion (1) using expressions for the stresses in terms of the displacement fields and identifying equal powers of ξ yields three recursion formulas for $u_{j+2}, v_{j+2}, w_{j+2}$. For u_{j+2} the relations are

$$\begin{aligned} u_{j+2} =& \frac{1}{R^2(j+1)(j+2)(\lambda+2\mu)}\Big[\rho\big(\frac{\partial^2 u_{j-2}}{\partial t^2} + 2R\frac{\partial^2 u_{j-1}}{\partial t^2} + R^2\frac{\partial^2 u_j}{\partial t^2}\big) \\ &-\mu\big(\frac{\partial^2 u_{j-2}}{\partial z^2} + 2R\frac{\partial^2 u_{j-1}}{\partial z^2} + R^2\frac{\partial^2 u_j}{\partial z^2} + \frac{\partial^2 u_j}{\partial \theta^2}\big) - (\lambda+2\mu)\big((j^2-1)u_j + R(j+1)(2j+1)u_{j+1}\big) \\ &-\big((j-1)\lambda + (j-3)\mu\big)\frac{\partial v_j}{\partial\theta} + R(j+1)(\lambda+\mu)\frac{\partial v_{j+1}}{\partial\theta} \\ &-(\lambda+\mu)\big((j+1)\frac{\partial w_{j-1}}{\partial z} + 2Rj\frac{\partial w_j}{\partial z} + R^2(j+1)\frac{\partial w_{j+1}}{\partial z}\big)\Big], \end{aligned} \tag{3}$$

for $j = 0, 1, \ldots$. Here $u_j, v_j, w_j \equiv 0$ for $j < 0$. Similar results are obtained for v_{j+2} and w_{j+2}. By using these recursion formulas, all subsequent expressions involving u_j, v_j, w_j with $j = \{2, 3, \ldots\}$ may thus be written in terms of u_j, v_j, w_j with $j = \{0, 1\}$. These relations are no further approximations, they stem from the definition of the series expansions (2) and are as such exact.

From now on, the outer and inner ring surfaces are assumed free: $\sigma_{rr} = \sigma_{r\theta} = \sigma_{rz} = 0$ for $\xi = \pm h/2$. It is convenient to express these boundary conditions in terms of the differences and sums of the surface stresses, as a common thickness factor (h) in the differences hereby can be cancelled out. Introduce $\Delta\sigma = \sigma(h/2,\theta,t) - \sigma(-h/2,\theta,t)$ and $\Sigma\sigma = \sigma(h/2,\theta,t) + \sigma(-h/2,\theta,t)$ where σ is either σ_{rr}, $\sigma_{r\theta}$ or σ_{rz}. Hence, the six boundary conditions are

$$\Delta\sigma_{rr} = 0, \quad \Delta\sigma_{r\theta} = 0, \quad \Delta\sigma_{rz} = 0, \quad \Sigma\sigma_{rr} = 0, \quad \Sigma\sigma_{r\theta} = 0, \quad \Sigma\sigma_{rz} = 0. \tag{4}$$

Using the series expansion (2) together with the recursion formulas (3) in the stress representations, it is straightforward to write the boundary conditions (4) in terms of the displacements u_j, v_j, w_j with $j = \{0, 1\}$. These partial differential equations are the sought new shell equations. When deriving the set of shell equations, the lengthy algebraic manipulations have been performed using the commercial code Mathematica[1].

Introducing the general matrix operator form $\mathcal{L}\vec{u} = \vec{0}$, the equation system becomes

$$\mathcal{L}_6\vec{u}_6 = \vec{0}, \tag{5}$$

where $\vec{u}_6 = (u_0, v_0, w_0, Ru_1, Rv_1, Rw_1)^T$. The six-by-six matrix operator $\mathcal{L}_6$ may be decomposed as

$$\mathcal{L}_6 = \mathcal{A}_6 + \eta\mathcal{B}_6 + \eta^2\mathcal{C}_6 + \ldots, \tag{6}$$

where $\eta = h^2/12R^2$ as only even powers in the thickness are present. Due to the way the boundary conditions are represented in $\mathcal{L}_6$, each matrix element involves either only odd spatial derivatives or only even spatial derivatives. The time derivatives are of even order throughout. When decomposing the operator $\mathcal{L}_6$ according to (6) the matrix corresponding to η^j involves derivatives up to order $2(j+1)$ in both space and time.

[1] Registered trademark of Wolfram Research Inc.

Note that so far no approximations have been performed. Moreover, the expansion system is believed to be asymptotically correct, see Section 4. The operator $\mathcal{L}_6$ may, in principle, be truncated to any order. However, the main interest here is to study lower order expansions as these are of most practical use.

While it is convenient to work in terms of the field $\vec{u}_6$ when calculating the displacements (2) adopting (3), it is of some interest to further reduce the number of fields. In order to make comparisons with classical bending theories, only the three fields u_0, v_0 and w_0 are to be retained, while comparisons with theories involving shearing and rotary inertia are carried out using the five fields u_0, v_0, w_0, v_1, w_1. Thus, in these cases the other fields may be eliminated by combining the equations in (5).

3 Eigenfrequencies for a ring

Consider a 2D circular ring in plane strain vibrating in the $(r\theta)$-plane, independent of the $z-$coordinate. Hence the fields w_0 and w_1 are hereby set to zero. In this section, the eigenfrequencies for the different approximate theories are compared with each other and the exact theory. Considering a fixed frequency ω, the displacement fields may be expressed in terms of Fourier series. Each mode of $\vec{u}_6$, now consisting of only four terms, has the following representation

$$\left.\begin{array}{ll} \{u_{j,0}(\omega)\mathrm{e}^{-\mathrm{i}\omega t}, & u_{j,m}(\omega)\cos m\theta \mathrm{e}^{-\mathrm{i}\omega t}\} \\ \{v_{j,0}(\omega)\mathrm{e}^{-\mathrm{i}\omega t}, & v_{j,m}(\omega)\sin m\theta \mathrm{e}^{-\mathrm{i}\omega t}\} \end{array}\right\} \quad j = 0, 1\,, \quad m = 1, 2 \ldots. \tag{7}$$

Consider the equation system (5) that is expressed in terms of the four fields u_0, v_0, u_1, v_1. Table 1 presents the three lowest nondimensional eigenfrequencies $\Omega = \omega R/c_E$ where $c_E = \sqrt{E/\rho}$, for each mode $m = 0, 1, 2, 3$ when $h/R = 1/5$. Here, the exact theory is compared to classical membrane theory, bending theory (Love), shearing and inertia theory (Naghdi and Cooper [5]) as well as the η^1 expansion theory. The comparisons are made in terms of the relative error. When the absolute value of the relative error is less than 10^{-7}, this is marked by a star $(*)$. It is clear from these tables that Naghdi-Cooper and the η^1 expansion theories are superior to the membrane and Love theories, as expected.

m	Ω	Exact	Membrane	Love	N-C	η^1
$m=0$	$\Omega_{0,1}$	1.0530381	-4.51×10^{-3}	-4.51×10^{-3}	-4.51×10^{-3}	1.99×10^{-5}
	$\Omega_{0,2}$	9.7533236	–	–	1.23×10^{-1}	-9.74×10^{-2}
	$\Omega_{0,3}$	9.8157302	–	–	1.47×10^{-1}	-9.16×10^{-2}
$m=1$	$\Omega_{1,1}$	0.62119597	-1.64×10^{-3}	–	-3.67×10^{-6}	-1.43×10^{-5}
	$\Omega_{1,2}$	1.4740323	5.74×10^{-3}	7.38×10^{-3}	-2.68×10^{-3}	1.58×10^{-5}
	$\Omega_{1,3}$	9.8860272	–	–	-1.35×10^{-1}	-9.53×10^{-2}
$m=2$	$\Omega_{2,1}$	0.15928015	–	-1.52×10^{-2}	-6.85×10^{-4}	-7.83×10^{-3}
	$\Omega_{2,2}$	1.2422917	-1.57×10^{-3}	–	1.54×10^{-5}	-3.41×10^{-5}
	$\Omega_{2,3}$	2.3178905	1.13×10^{-2}	1.56×10^{-2}	-7.04×10^{-4}	2.59×10^{-4}
$m=3$	$\Omega_{3,1}$	0.43675502	–	4.60×10^{-2}	4.80×10^{-3}	-6.66×10^{-3}
	$\Omega_{3,2}$	1.8631873	-1.43×10^{-3}	–	4.72×10^{-5}	-5.02×10^{-5}
	$\Omega_{3,3}$	3.2676316	1.45×10^{-2}	2.01×10^{-2}	1.44×10^{-3}	3.20×10^{-4}

Table 1: The eigenfrequencies for exact theory and the relative error for membrane, Love, Naghdi-Cooper (N-C) and series expansions η^1 theories for $h/R = 1/5$. N-C with $\kappa^2 = 5/6$.

4 Dispersion Relations

The performance of the 3D series expansion shell equations has been validated using the dispersion relations for waves traveling along the cylinder, parallel to the z-axis, with wavenumber k. It is noted that for $k = 0$, this yields the two-dimensional eigenfrequencies for a circular ring in plain strain as treated in the previous

section. As for the 2D ring case, a fixed frequency ansatz is made and the dependency on θ is assumed to be of a Fourier series type with factors like $\sin m\theta$. It should be stressed here that by expanding the exact dispersion equation in power series in terms of nondimensional wavenumber kR, each term is identical to the corresponding term according to the present theory, at least for the lowest terms studied (see comparable situation for plates by Losin [3]).

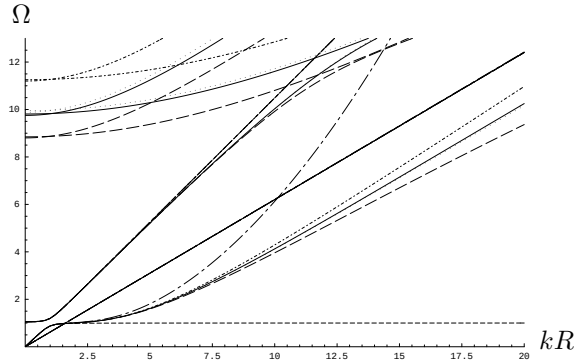

Figure 1: Dispersion curves for modes with $m = 0$; $h/R = 1/5$. Solid lines represent the exact solution, short dashes η^0, long dashes η^1, small dots η^2, long dash-dotted Love and short dash-dotted Naghdi-Cooper.

In Figure 1 the dispersion curves are plotted for the thick-walled case of $h/R = 1/5$, for different $m = 0$. All solutions that fit in the range shown are also plotted. The straight lines starting from the origin represent the uncoupled torsional wave mode, accurately predicted by all theories, as expected given its dispersion-free nature. The other curves emanating from the origin represent the longitudinal rod mode. Note that the η^0-solution starts off well, but shows no stiffening with raised wave numbers above approximately $kR = 1.5$. The Love solution departs visibly from the correct solution at about $kR = 3$. The η^1 and N-C solutions show similar performance, although it can be noted that while the former tends to be too soft, the latter is too stiff in this mode.

References

[1] A. Boström. On wave equations for elastic rods. *Z. Angew. Math. Mech.*, 80:245–251, 2000.

[2] A. Boström, G. Johansson, and P. Olsson. On the rational derivation of a hierarchy of dynamic equations for a homogeneous, isotropic, elastic plate. *Int. J. Solids Struct.*, 38:2487–2501, 2001.

[3] N.A. Losin. On the equivalence of dispersion relations resulting from Rayleigh-Lamb frequency equation and the operator plate model. *J. Vibr. Acoust.*, 123:417–420, 2001.

[4] K. Mauritsson, A. Boström, and P.D. Folkow. Modelling of thin piezoelectric layers on plates. *Accepted for publication in Wave Motion*, 2008.

[5] P.M. Naghdi and R.M. Cooper. Propagation of elastic waves in cylindrical shells, including the effects of transverse shear and rotatory inertia. *J. Acoust. Soc. Am.*, 28:56–63, 1956.

Proceedings of the 6th International Conference on
Computation of Shell and Spatial Structures
IASS-IACM 2008: Spanning Nano to Mega
28-31 May 2008, Cornell University, Ithaca, NY, USA
John F. ABEL and J. Robert COOKE (eds.)

Dynamic equations for a homogenous, fully anisotropic, elastic plate

Karl MAURITSSON*, Anders BOSTRÖM, Peter D. FOLKOW

* Department of Applied Mechanics, Chalmers University of Technology, SE-412 96 Göteborg, Sweden

Abstract

The derivation of plate equations for a homogenous, fully anisotropic, elastic plate is considered. Power series expansions in the thickness coordinate for the displacements lead to recursion relations among the expansion functions. Using these in the boundary conditions a set of plate equations, which can be truncated to any order in the thickness, are obtained and it is believed that these equations are asymptotically correct. Numerical investigations for guided waves along the plate illustrate the accuracy.

1 Introduction

Dynamic plate equations for a homogenous, fully anisotropic, elastic plate are derived by a systematic power series expansion approach, previously adopted for isotropic plates by Boström *et al*. [2] and for piezoelectric layers by Mauritsson *et al*. [3]. One advantage with the consideration of a material without any symmetry classes is that all other cases can be obtained as special cases. As the stiffness matrix for a fully anisotropic material includes 21 independent stiffness constants, the explicit expressions for the coefficients in the plate equations become very complicated. Of this reason the plate equations for the most general case are derived on a very compact form as two matrix equations, including matrix operators that are recursively defined. To derive the plate equations on matrix form, all field quantities and equations are expressed with abbreviated subscripts, according to Auld [1]. The displacement components are then expanded in power series in the thickness coordinate. Insertion of these expansions in the three-dimensional equations of motion leads to recursion relations among the expansion functions, which can be used to eliminate all but some of the lowest-order expansion functions. The power series expansions are also inserted in the boundary conditions at the top and the bottom of the plate and by using the recursion relations two matrix equations are obtained. These represent a set of six scalar equations of motion, including six unknown expansion functions. The plate equations can be truncated to any order in the thickness and it is believed that the equations are asymptotically correct. For the special case of an orthotropic material, the six plate equations can be added and subtracted pair wise to obtain two uncoupled systems of equations, each of them including three equations and three unknowns. The two uncoupled systems correspond to the symmetric and antisymmetric part of the motion, respectively. The three equations corresponding to the antisymmetric motion of the orthotropic plate are explicitly given to quadratic order in the thickness, which is necessary to account for the bending stiffness. All lengthy analytical calculations involved are performed with the commercial code Mathematica[1]. To validate the orthotropic plate equations dispersion curves for some numerical examples are determined and compared with dispersion curves from exact three-dimensional theory. Comparisons are also made with some other approximate theories.

[1] Registered trademark of Wolfram Research Inc.

2 Problem formulation

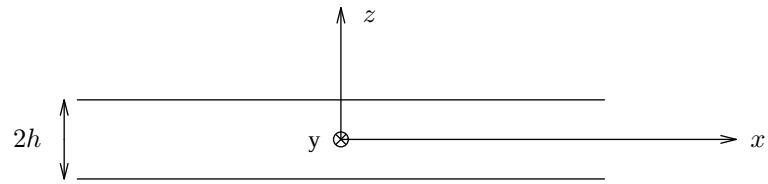

Figure 1: The geometry.

Consider a rectangular plate of thickness $2h$ according to Figure. 1. The plate is homogenous, fully anisotropic and linearly elastic with density ρ and a stiffness matrix which includes 21 independent stiffness constants

$$[c_{IJ}] = \begin{pmatrix} c_{11} & c_{12} & c_{13} & c_{14} & c_{15} & c_{16} \\ c_{12} & c_{22} & c_{23} & c_{24} & c_{25} & c_{26} \\ c_{13} & c_{23} & c_{33} & c_{34} & c_{35} & c_{36} \\ c_{14} & c_{24} & c_{34} & c_{44} & c_{45} & c_{46} \\ c_{15} & c_{25} & c_{35} & c_{45} & c_{55} & c_{56} \\ c_{16} & c_{26} & c_{36} & c_{46} & c_{56} & c_{66} \end{pmatrix}. \tag{1}$$

A coordinate system is introduced with the x and y axes in the horizontal middle plane and the z axis in the vertical direction. The displacement components in the x, y and z direction, respectively, are collected in a three-element column matrix as

$$[u_i] = \begin{pmatrix} u & v & w \end{pmatrix}^T, \tag{2}$$

while the stress is written as a six-element column matrix

$$[T_I] = \begin{pmatrix} T_{xx} & T_{yy} & T_{zz} & T_{yz} & T_{xz} & T_{xy} \end{pmatrix}^T. \tag{3}$$

The divergence of stress operator, ∇_{iJ}, and the symmetric gradient operator, ∇_{Ij}, are defined by the following matrix representations

$$[\nabla_{iJ}] = \begin{pmatrix} \partial_x & 0 & 0 & 0 & \partial_z & \partial_y \\ 0 & \partial_y & 0 & \partial_z & 0 & \partial_x \\ 0 & 0 & \partial_z & \partial_y & \partial_x & 0 \end{pmatrix}, \qquad [\nabla_{Ij}] = [\nabla_{iJ}]^T. \tag{4}$$

For a linearly elastic material the stress is related to the displacement by the following relation, using abbreviated subscripts

$$T_I = c_{IJ}\nabla_{Jk}u_k, \tag{5}$$

and the equations of motion are written

$$\nabla_{iJ}c_{JK}\nabla_{Kl}u_l = \rho\partial_t^2 u_i. \tag{6}$$

3 Plate equations

The displacement components are expanded in power series like

$$u_i(x,y,z,t) = \sum_{n=0}^{\infty} z^n u_i^{(n)}(x,y,t), \tag{7}$$

where $u_i^{(n)}(x,y,t)$ with components $u_n(x,y,t)$, $v_n(x,y,t)$, $w_n(x,y,t)$ are expansion functions independent of z.

Insertion of the series expansions (7) in the equations of motion (6) gives the following recursion relation

$$u_i^{(n+2)} = \frac{1}{(n+1)(n+2)} M_{ij}\left[\rho\ddot{u}_j^{(n)} - \overline{\nabla}_{jK}c_{KL}\overline{\nabla}_{Lm}u_m^{(n)} - (n+1)(L_{jK}c_{KL}\overline{\nabla}_{Lm} + \overline{\nabla}_{jK}c_{KL}L_{Lm})u_m^{(n+1)}\right]. \tag{8}$$

The matrix operators with an overline, $\overline{\nabla}_{iJ}$ and $\overline{\nabla}_{Ij}$, respectively, are the same as ∇_{iJ} and ∇_{Ij}, but with all derivatives with respect to z put to zero, i.e. $\partial_z = 0$. Also the following matrices were introduced

$$[C_{ij}] = \begin{pmatrix} c_{55} & c_{45} & c_{35} \\ c_{45} & c_{44} & c_{34} \\ c_{35} & c_{34} & c_{33} \end{pmatrix}, \qquad [M_{ij}] = [C_{ij}]^{-1}, \tag{9}$$

$$[L_{iJ}] = \begin{pmatrix} 0 & 0 & 0 & 0 & 0 & 1 \\ 0 & 0 & 0 & 0 & 1 & 0 \\ 0 & 0 & 0 & 1 & 0 & 0 \end{pmatrix}, \qquad [L_{Ij}] = [L_{iJ}]^T. \tag{10}$$

The recursion relation can be used to express all expansion functions in the lowest-order ones with an upper index $n = 0, 1$. The recursion relation (8) can then be rewritten as

$$u_i^{(n)} = \frac{1}{n!}\big[A_{ij}^{(n-2)} u_j^{(0)} + B_{ij}^{(n-2)} u_j^{(1)}\big], \tag{11}$$

where the differential operators $A_{ij}^{(n)}$ and $B_{ij}^{(n)}$ are recursively defined in the following way

$$\begin{aligned} &A_{ij}^{(-2)} = \delta_{ij}, \qquad A_{ij}^{(-1)} = 0, \qquad A_{im}^{(0)} = M_{ij}(\delta_{jm}\rho\partial_t^2 - \overline{\nabla}_{jK} c_{KL} \overline{\nabla}_{Lm}), \\ &A_{ik}^{(n)} = B_{ij}^{(0)} A_{jk}^{(n-1)} + A_{ij}^{(0)} A_{jk}^{(n-2)}, \quad n = 1, 2, \dots, \end{aligned} \tag{12}$$

$$\begin{aligned} &B_{ij}^{(-2)} = 0, \qquad B_{ij}^{(-1)} = \delta_{ij}, \qquad B_{im}^{(0)} = -M_{ij}(L_{jK} c_{KL} \overline{\nabla}_{Lm} + \overline{\nabla}_{jK} c_{KL} L_{Lm}), \\ &B_{ik}^{(n)} = B_{ij}^{(0)} B_{jk}^{(n-1)} + A_{ij}^{(0)} B_{jk}^{(n-2)}, \quad n = 1, 2, \dots, \end{aligned} \tag{13}$$

where $[\delta_{ij}]$ is the identity matrix. Insertion of the power series expansions (7) in the stress relation (5) gives

$$T_I = c_{IJ} \sum_{n=0}^{\infty} z^n \big[(n+1) L_{Jk} u_k^{(n+1)} + \overline{\nabla}_{Jk} u_k^{(n)}\big]. \tag{14}$$

At the top and the bottom of the plate ($z = \pm h$), the traction T_i, where $[T_i] = (\ T_{zz} \quad T_{yz} \quad T_{xz}\ )^T$, is specified as T_i^T and T_i^B, respectively. Insertion of the recursion relation (11) in the expanded stress relation (14) and use of the boundary conditions then gives the following two matrix relations

$$\begin{aligned} &c_{IJ} \sum_{n=0}^{\infty} \frac{h^n}{n!} \big[(L_{Jk} A_{kl}^{(n-1)} + \overline{\nabla}_{Jk} A_{kl}^{(n-2)}) u_l^{(0)} + (L_{Jk} B_{kl}^{(n-1)} + \overline{\nabla}_{Jk} B_{kl}^{(n-2)}) u_l^{(1)}\big] = T_i^T, \\ &c_{IJ} \sum_{n=0}^{\infty} \frac{(-h)^n}{n!} \big[(L_{Jk} A_{kl}^{(n-1)} + \overline{\nabla}_{Jk} A_{kl}^{(n-2)}) u_l^{(0)} + (L_{Jk} B_{kl}^{(n-1)} + \overline{\nabla}_{Jk} B_{kl}^{(n-2)}) u_l^{(1)}\big] = T_i^B, \end{aligned} \tag{15}$$

where $I = 3, 4, 5,\ \ i = 1, 2, 3$. Each matrix equation corresponds to three scalar plate equations, so there is a total of six plate equations expressed in six unknown components of expansion functions ($u_0, v_0, w_0, u_1, v_1, w_1$). For the special case of an orthotropic material the six equations can be added and subtracted pairwise to obtain a decouple in the symmetric and antisymmetric part of the motion. The three plate equations corresponding to the antisymmetric motion of an orthotropic plate are truncated to quadratic order in the thickness and given by

$$\begin{aligned} &A_{000} u_1 + A_{100} \partial_x w_0 + h^2 \big[A_{002} \partial_t^2 u_1 + A_{200} \partial_x^2 u_1 + A_{020} \partial_y^2 u_1 \\ &\quad + A_{110} \partial_x \partial_y v_1 + A_{102} \partial_x \partial_t^2 w_0 + A_{300} \partial_x^3 w_0 + A_{120} \partial_x \partial_y^2 w_0\big] = T_{xz}, \end{aligned} \tag{16}$$

$$\begin{aligned} &B_{000} v_1 + B_{010} \partial_y w_0 + h^2 \big[B_{002} \partial_t^2 v_1 + B_{020} \partial_y^2 v_1 + B_{200} \partial_x^2 v_1 \\ &\quad + B_{110} \partial_x \partial_y u_1 + B_{012} \partial_y \partial_t^2 w_0 + B_{030} \partial_y^3 w_0 + B_{210} \partial_x^2 \partial_y w_0\big] = T_{yz}, \end{aligned} \tag{17}$$

$$\begin{aligned} &h[C_{002} \partial_t^2 w_0 + C_{200} \partial_x^2 w_0 + C_{020} \partial_y^2 w_0 + C_{100} \partial_x u_1 + C_{010} \partial_y v_1] \\ &\quad + h^3 \big[C_{004} \partial_t^4 w_0 + C_{202} \partial_x^2 \partial_t^2 w_0 + C_{022} \partial_y^2 \partial_t^2 w_0 + C_{400} \partial_x^4 w_0 + C_{040} \partial_y^4 w_0 + C_{220} \partial_x^2 \partial_y^2 w_0 \\ &\qquad + C_{102} \partial_x \partial_t^2 u_1 + C_{300} \partial_x^3 u_1 + C_{120} \partial_x \partial_y^2 u_1 + C_{012} \partial_y \partial_t^2 v_1 + C_{030} \partial_y^3 v_1 + C_{021} \partial_x^2 \partial_y v_1\big] = T_{zz}, \end{aligned} \tag{18}$$

where A_{ijk}, B_{ijk} and C_{ijk} are material constants including the density and stiffness components.

4 Dispersion relations

The orthotropic plate equations have been validated by investigating dispersion relations for time harmonic waves with frequency ω propagating along different directions in the xy plane. Comparisons have been made with dispersion relations from exact three-dimensional theory and some other approximate theories. Here consider waves propagating in the x direction in a graphite-epoxy (AS/3501) plate. In Figure 2 dispersion curves from asymptotic plate theory, exact theory and a Mindlin theory for orthotropic plates (see [4]) are shown. The dimensionless frequency $\Omega = \omega h\sqrt{\rho/(\lambda + 2\mu)}$ is plotted versus dimensionless wave number kh, where k is the wave number in the direction of propagation. The dispersion curves shows that the developed theory very well approximates the exact theory at low frequencies and for large wave numbers the second mode is better approximated by the asymptotic plate equations than by Mindlin theory.

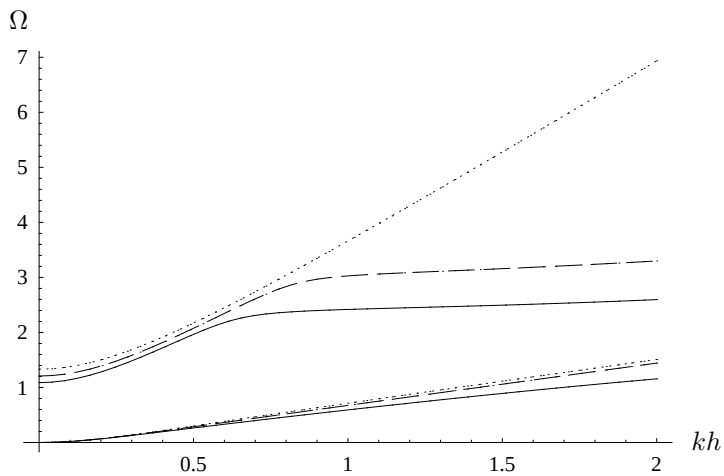

Figure 2: Dispersion curves comparing asymptotic plate equation (full-drawn), Mindlin (dotted) and exact (dashed) solutions.

References

[1] B.A. Auld. *Acoustic Fields and Waves in Solids*. Krieger, Malabar, FL, 1990.

[2] A. Boström, G. Johansson, P. Olsson. *On the rational derivation of a hierarchy of dynamic equations for a homogeneous, isotropic, elastic plate*. Int. J. Solids Struct., 38:2487–2501, 2001.

[3] K. Mauritsson, A. Boström, P.D. Folkow. *Modelling of thin piezoelectric layers on plates*. Wave Motion, 45:616–628, 2008.

[4] Y. Yi-Yuan. *Vibrations of Elastic Plates*. Springer-Verlag, New York, 1996.